Acta Montanistica Slovaca
ISSN 1335-1788
actamont.tuke.sk

Assessment of Petrographic and Physico-Mechanical Properties of Granodiorites for Aggregate Usage: A Comprehensive Case Study from Mayar, Dir (Lower), Khyber Pakhtunkhwa Pakistan

Farhat ULLAH[1,2], Rehan KHAN[1,2], Asad MUHAMMAD[1,2], Ihtisham ISLAM[3,4], Abdul Rahim ASIF[4], Qarib ULLAH[1] and Salman KHURSHID[1,2]*

Authors' affiliations and addresses:
[1] Department of Geology, University of Malakand (18800), Dir (Lower), Khyber Pakhtunkhwa, Pakistan
e-mail: farhatgeo1@gmail.com
e-mail: rkgeo7262@gmail.com
e-mail: asad@uom.edu.pk
e-mail: qaribullahuom@gmail.com
e-mail: salmankhurshid@uom.edu.pk

[2] Department of Earth Sciences, Quaid-i-Azam University, Islamabad (45320), Pakistan

[3] Department of Geology, Shaheed Benazir Bhutto University, Sheringal (18050), Pakistan
e-mail: ihtisham.islam@sbbu.edu.pk

[4] National Centre of Excellence in Geology, University of Peshawar (25130), Pakistan
e-mail: abdulrahimasif@yahoo.com

***Correspondence:**
Asad Muhammad, Department of Geology, University of Malakand (18800), Dir (Lower), Khyber Pakhtunkhwa, Pakistan
tel.: +923339152036
e-mail: asad@uom.edu.pk

Acknowledgement:
The authors would like to acknowledge the National Centre of Excellence in Geology, University of Peshawar (Pakistan) for providing laboratory facilities.

How to cite this article:
Ullah, F., Khan, R., Muhammad, A., Islam, I., Asif, A.R, Ullah, Q. and Khurshid, S. (2025). Assessment of Petrographic and Physico-Mechanical Properties of Granodiorites for Aggregate Usage: A Comprehensive Case Study from Mayar, Dir (Lower), Khyber Pakhtunkhwa Pakistan. *Acta Monstanistica Slovaca,* Volume 30 (2), 492-508

DOI:
https://doi.org/10.46544/AMS.v30i2.17

Abstract
The current study systematically evaluates the granodiorites from the Mayar area through integrated petrographic and physico-mechanical analyses as well as the interrelationship between these parameters to assess their viability as heavyweight aggregates and dimensions stones in civil engineering applications. Field observations indicate that the rock is medium to coarse-grained, hard, and compact, having dark brown and greyish colour on weathered and fresh surfaces, respectively. Petrographic study exhibits that the rocks are euhedral to anhedral, having the dominant concentrations of plagioclase, quartz, K-feldspar, biotite, hornblende, fluorite, and andalusite, with a minor amount of clinopyroxene, muscovite, rutile, and actinolite. The physical and mechanical characterization includes grading, specific gravity and absorption, flakiness and elongation indices, Los Angeles abrasion, and soundness. These analyses demonstrate compliance with standard permissible ranges, confirming their potential as construction materials. Mechanical analysis yields average uniaxial compressive strength (UCS) and uniaxial tensile strength (UTS) 52.96 MPa and 8.54 MPa, respectively, classifying the rock within the moderate to strong category. The above-integrated study reveals that medium-grained granodiorites exhibit higher strength compared to coarse-grained varieties. Plagioclase and mica contents are identified as the dominant controlling factors, whereas quartz and K-feldspar show negligible influence on the strength of the granodiorite. Considering the favourable mechanical properties, excellent and extensive exposure and logistical accessibility of the outcrop, it is concluded that the granodiorite of the Mayar area is recommended for high-load-bearing applications, including Dir- Chitral motorway, CPEC developmental schemes, railway ballast, highways, and dimension stone cladding. Moreover, the quarry byproducts can be utilized as sustainable aggregates in secondary construction applications.

Keywords
CPEC; Construction materials; Aggregates; Granodiorite; Mechanical properties

© 2025 by the authors. Submitted for possible open access publication under the terms and conditions of the Creative Commons Attribution (CC BY) license (http://creativecommons.org/licenses/by/4.0/).

Introduction

The Mayar Granodiorite, part of the Kohistan Island Arc (KIA), is a valuable source of construction materials, making it essential to explore its properties and potential for infrastructure projects. The Kohistan Island rocks are used for several purposes, i.e. construction materials, building facades, paving, and dimension stones. Their physical and chemical properties are controlled by their origin, petrography, weathering, and alteration (Asif et al., 2021; Khattak et al., 2021; Siegesmund et al., 2022; Shah et al., 2024). Their evaluation potential for use as construction material must be helpful from their petrography and field investigation (Hussain et al., 2022; Asif et al., 2022; 2024). The study area is a part of the Kohistan Island Arc, and the igneous rocks can be used as an excellent source of construction materials because they are generally hard, compact, and less fractured. The pores in the extrusive igneous rocks, fractures, and cleaves increase the absorption ability and hence badly affect its capability to be used as construction materials (Adomako et al., 2021).

The main objective of this current study is to determine the petrography and suitability of the granodiorite to use as construction materials due to the current increase in construction activity, such as the expansion of roads, reconstructions of buildings, highways, bridges, and dams, which were severely affected by the August 2022 floods in Pakistan.

The floods that hit Pakistan in August 2022 were devastating, affecting over 33 million people, with nearly 1,700 lives lost (Sawa, 2023). More than 1.8 million homes were damaged or destroyed, and approximately one-third of the country's land area, around 170,000 square kilometres, was submerged (Aman et al., 2025). The flooding severely damaged infrastructure, including roads, bridges, and dams, creating an urgent need for durable and readily available construction materials for rebuilding efforts. The total damage from the floods is estimated to exceed $30 billion, causing widespread economic disruption (Nanditha et al., 2023). This has driven a sharp increase in demand for materials like aggregates, which are needed to restore critical infrastructure such as roads, highways, and flood-affected areas. Therefore, need to explore more quarries of rocks that are easily accessible, feasible, and available to use for construction purposes to overcome the demand for aggregates.

The future outcome of this research may lead to substituting the granodiorite with granite, sandstone, and limestone. The study area is 34°54′54″N and 71°36′57″E are located on the western side of Timergara (Fig. 1). The distance from Timergara to Kotkay Mayar is about 33.4 km and 1 km westward from G.T. Road Maskini, Dir Lower.

Geology and Tectonics

The northern areas of Pakistan consist of three parts: the Eurasian plate in the north, the Kohistan Island Arc (KIA) in the middle, and the Indian plate in the south. The KIA is one of the most complete sections of the island arc from the lower crust and adjoining mantle to the upper crust (Petterson, 2010). The KIA is sutured between the Shyok Suture Zone to the north and the Indus Tsangpo Suture Zone to the south (Baig et al., 2021). This cretaceous intra-oceanic island arc begins with the Indian plate northward drifting (Hu, Haoyui et al., 2020). The KIA represents the different tectonic stratigraphic units from south to north, including Jijal Complex, Kamila Amphibolite, Chillas Complex, Kohistan Batholith, Gilgit Gneisses, Chalt Volcanics and Yasin Group (Naseem et al., 2023). Dir Group is a 120 km long and 15-20 km wide belt that runs through Dir Swat valley in western Kohistan. The Dir Group is further divided into the Baraual Banda Slate Formation and Utror Volcanic Formation. The thickness of the Baraual Banda Slate is about 3 km. The lower part of the Baraual Banda Slate contains conglomerates, breccia, and pebbly sandstone, while the upper part is composed of thin-bedded sandstone, siltstone, and mudstone (Rashid et al., 2019). Rare interbedded limestone in Baraual Banda slate contains the marine faunas of the Late Paleocene age (Rashid et al., 2019). The Dir Utror Formation consists of basalt, basaltic andesite, dacite, rhyolite, pyroclastic breccia and tuff of calc-alkaline nature.

The study area is believed to be part of the Kamila amphibolite southern section extended to Afghanistan (Ullah et al., 2025). The dominant lithology Kamila amphibolite exposed in Dir Lower is dominantly amphibolite, having the inclusion of granite, granodiorite, hornblendite, diorite, quartz diorite, Porphyry quartz monzonite and gabbronorite (Ullah et al., 2025).

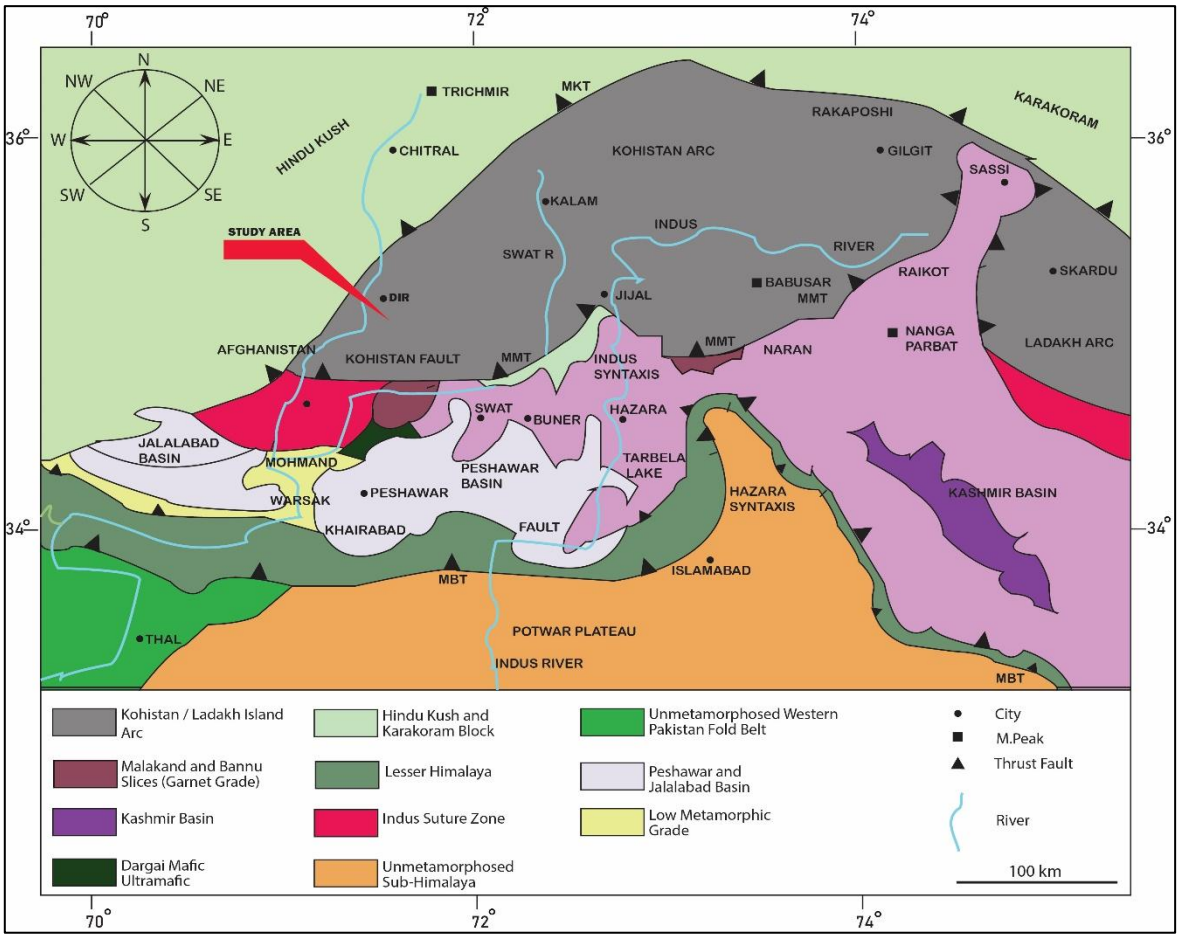

Fig. 1. Geological map of the North-western Himalayas showing the study area (after Ahmad et al., 2003).

Material and Methods

Field Observations

The rocks present in the studied area are medium to coarse-grained and have no fractures. Its colour is greyish and light to dark brown on fresh and weather surfaces, respectively(Fig. 2 c-d). The rocks are weathered, having dissolution of mica at latitude 34°54′55″N and longitude 71°36′ 57″ E (Fig. 2 c). In some places, rocks with spheroidal weathering can be seen (Fig. 2 a). In many places, there are alternate shared and compacted zones(Fig. 2e). Veins are present that vary in size, ranging from small, thin veins to large, thick bodies. The principal composition of the veins is quartz, feldspar, muscovite, and some minor amounts of biotite (Fig. 2f).

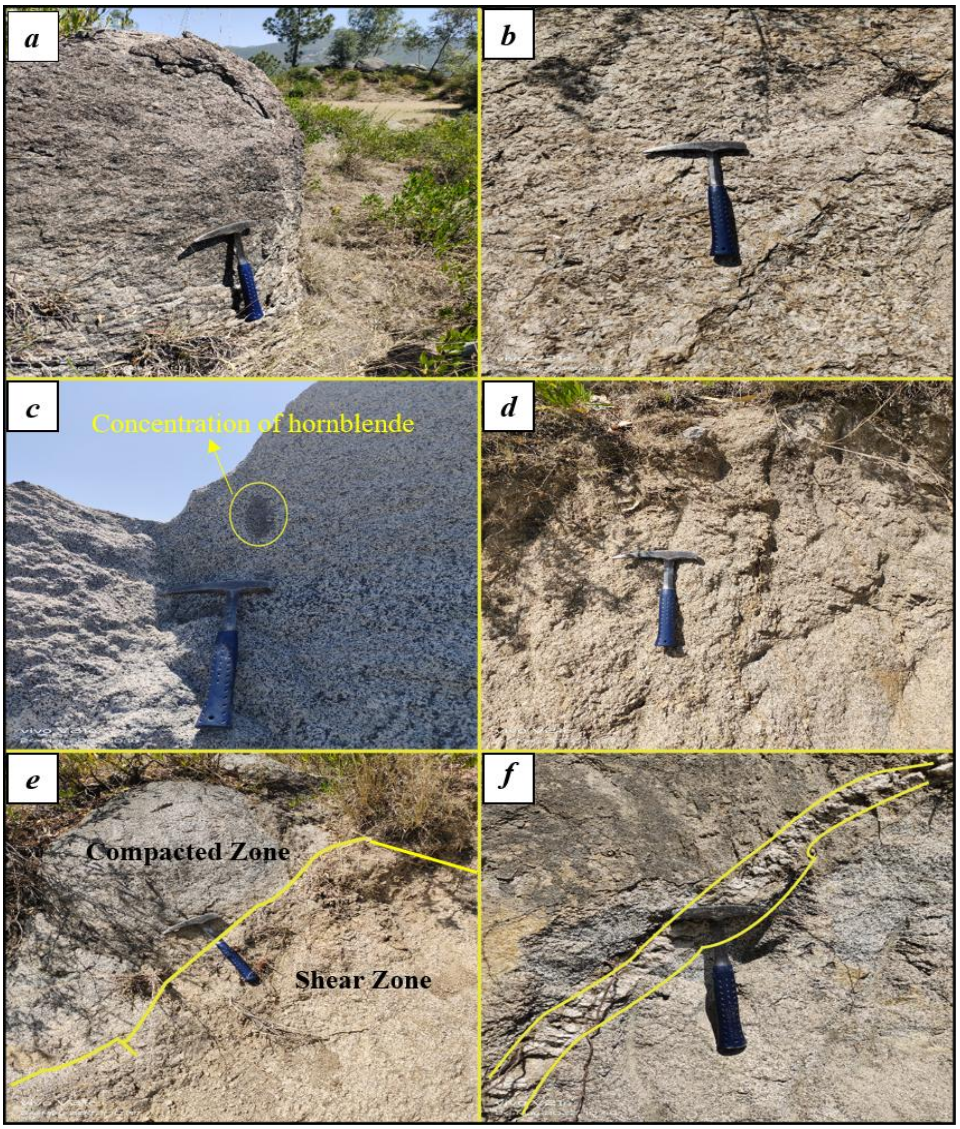

Fig. 2. Figure showing different outcrop features (a) Spheroidal Weathering (b) Dissolution of mica (c) Fresh surface having a concentration of hornblende (d) weathering of the Granodiorite (e) Alternate Shear and compacted zone (f) Granodiorite having quartz, feldspars veins

Laboratory Testing

Fieldwork is conducted in the study area to collect rock samples. Field photographs of important features are captured. Twelve different granodiorite rock samples are collected based on colour and textural variations, with ten representative samples selected for petrographic study. Thin sections are prepared in the rock-cutting Laboratory, Department of Geology, Bacha Khan University Charsadda. Photomicrographs of these thin sections are taken and examined in the Sedimentology Laboratory, NCE in Geology, University of Peshawar. Rock samples collected during fieldwork are analyzed according to international standards such as ASTM to determine physical and mechanical properties at the Geotechnical laboratory, NCE in Geology, University of Peshawar. This analysis includes Grading, Specific Gravity and Absorption, Elongation and Flakiness Index, Los Angeles Abrasion test, Soundness, Unconfined Compressive Strength (UCS), and Unconfined Tensile Strength (UTS).

Results and Discussion

Petrography

The dominant mineral compositions of the studied thin sections are plagioclase, quartz, K-feldspar, biotite hornblende, and andalusite. The minor minerals include zircon, rutile, clinopyroxene, fluorite, actinolite, and muscovite. Texturally, the rocks are coarse-grained, sub-equigranular to in-equigranular, and have sufficient dark-coloured minerals. Plagioclase is the most common mineral series present in the observed thin sections, ranging from 20 to 44.75%. The several plagioclase crystals show Carlsbad and polysynthetic twinning (Fig. 4a). The

lamellar twinning is also observed in thin sections (Fig. 4i). These crystals are subhedral to anhedral having a perfect set of cleavages with the inclusion of some fresh quartz and biotite (Fig. 4i). Quartz is another key mineral encountered during petrographic study. The range of quartz in different thin sections ranges from 18.75 to 26.75%. They are mostly anhedral, having a hypidiomorphic texture, and less commonly display undulose extinction in some thin sections (Fig. 4d). It is yellowish in colour, having fractures indicating highly strained conditions, and these fractures may include some fresh white colour quartz. Ribbon quartz is also observed to reveal strained conditions (Fig. 4d). Some unstrained quartz crystals are also present (Fig. 4 h). Another major mineral is K-feldspar, which ranges from 6.25 to 14.25%. They are subhedral to anhedral, having cleavages. It is usually present in silica-rich rocks but can also be found in intermediate rocks. Its relief is low, having a first-order grey interference colour. Biotite ranges from 7.75 to 15.25%, having a dark brown colour with some cleavages and well-developed flakes (Fig. 4c). Hornblende was present, which ranges from 2.25 to 9.50%. They have moderate relief, green and yellowish green to bluish green in colour. Most andalusites are anhedral, having cleavages and ranging from 2 to 12.75% (Fig. 4e). It is a stable mineral in strained conditions. Clinopyroxene ranges from 3 to 7.75% with anhedral crystals. It is common in intermediate igneous rocks and present in granodioritic rocks. Fluorites are euhedral to anhedral crystals usually present in the veins. The fluorite veins have biotite cross-cutting the quartz (Fig. 4k). The fluorite ranges from 3.25 to 19.75% but is absent in some thin sections. They are isotropic and usually the late minerals in the granitic type rocks. Muscovite ranges from 0.75 to 7.50%. In plutonic rocks, the mica is present together with quartz, plagioclase, and biotite. They have low relief with some cleavages. Rutile is present as an accessory mineral ranging from 0.50 to 3.75%. Its relief is high and coarse-grained, and cleavages can be seen (Fig. 4e). Zircon, as an accessory mineral present in many igneous and metamorphic rocks (Fig. 4f). The range of zircon is from 5 to 8.25%. Actinolite, another accessory mineral (0.50%), is only present in one thin section. The visual estimation of the abundant minerals (plagioclase, quartz, and k-feldspar) is illustrated by plotting them on the appropriate IUGS classification diagrams. The studied rock samples fall within the granodiorite portion of the said diagram.

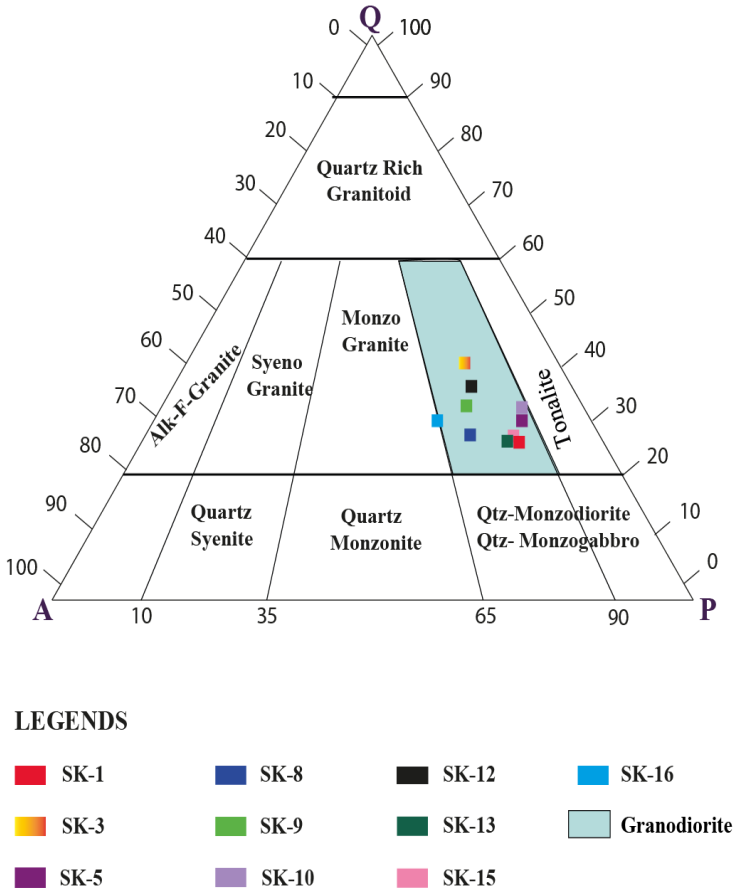

Fig. 3. Model composition of the studied Granodiorite rocks plotted on the IUGS classification diagram (from Le Maitre, 2002).

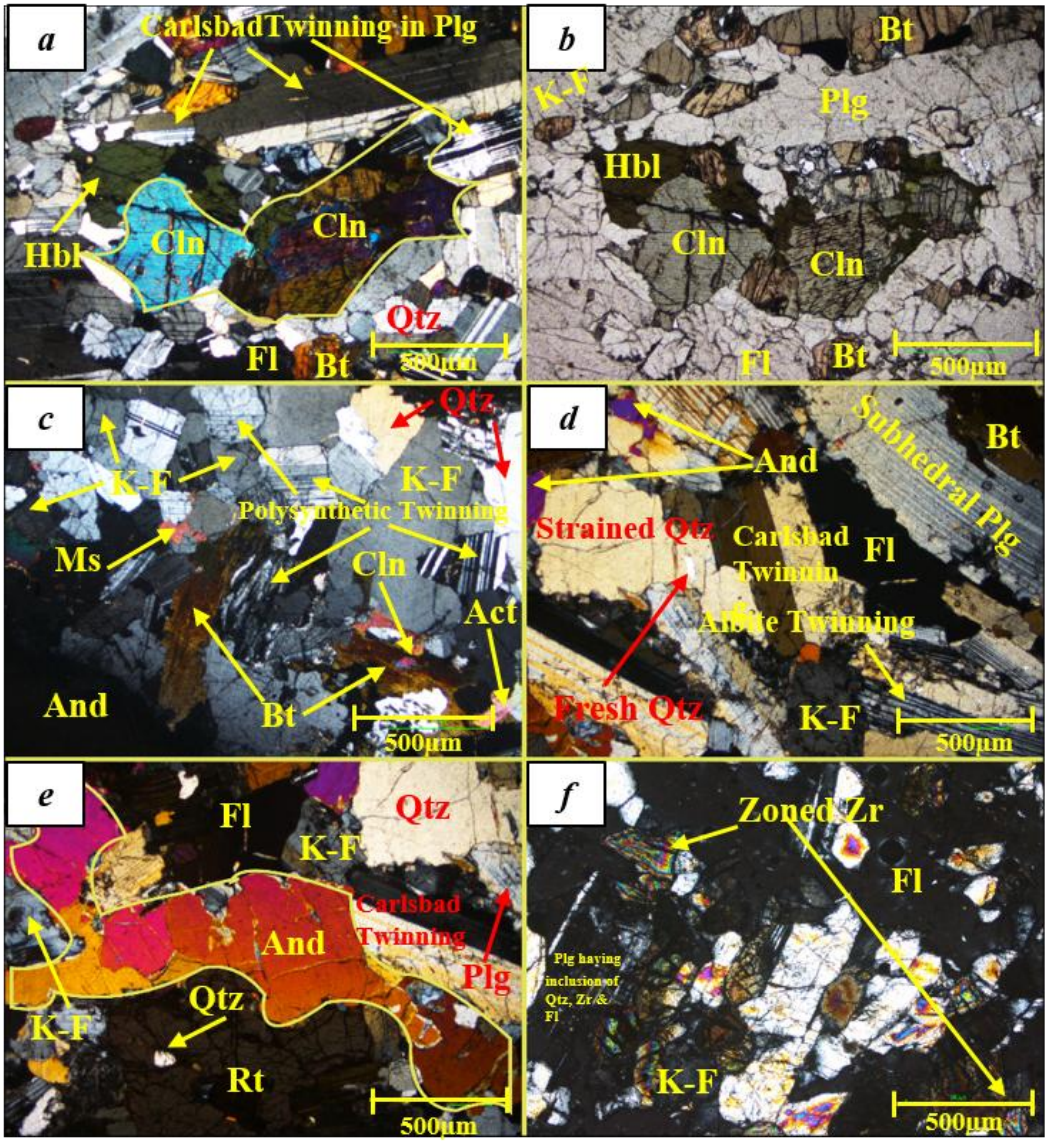

Fig. 4. Photomicrographs illustrating (a) Carlsbad Twinning in Plagioclase, different colours of clinopyroxene (XPL), (b) PPL view of the clinopyroxene, (c) Polysynthetic Twinning, strained quartz and flakes of biotite, (d) strained quartz having inclusion of fresh quartz, subhedral plagioclase, hypidiomorphic texture, (e) andalusite, rutile and quartz, (f) zoned zircon and plagioclase having inclusion of quartz zircon and fluorite. Key: Plg, Plagioclase; Qtz, Quartz; K-F, K-Feldspar; Bt, Biotite, Hbl, Hornblende; Cln, Clinopyroxene; Rt, Rutile; Fl, Fluorite; Ms, Muscovite And, Andalusite Zr, Zircon; Act, Actinolite)

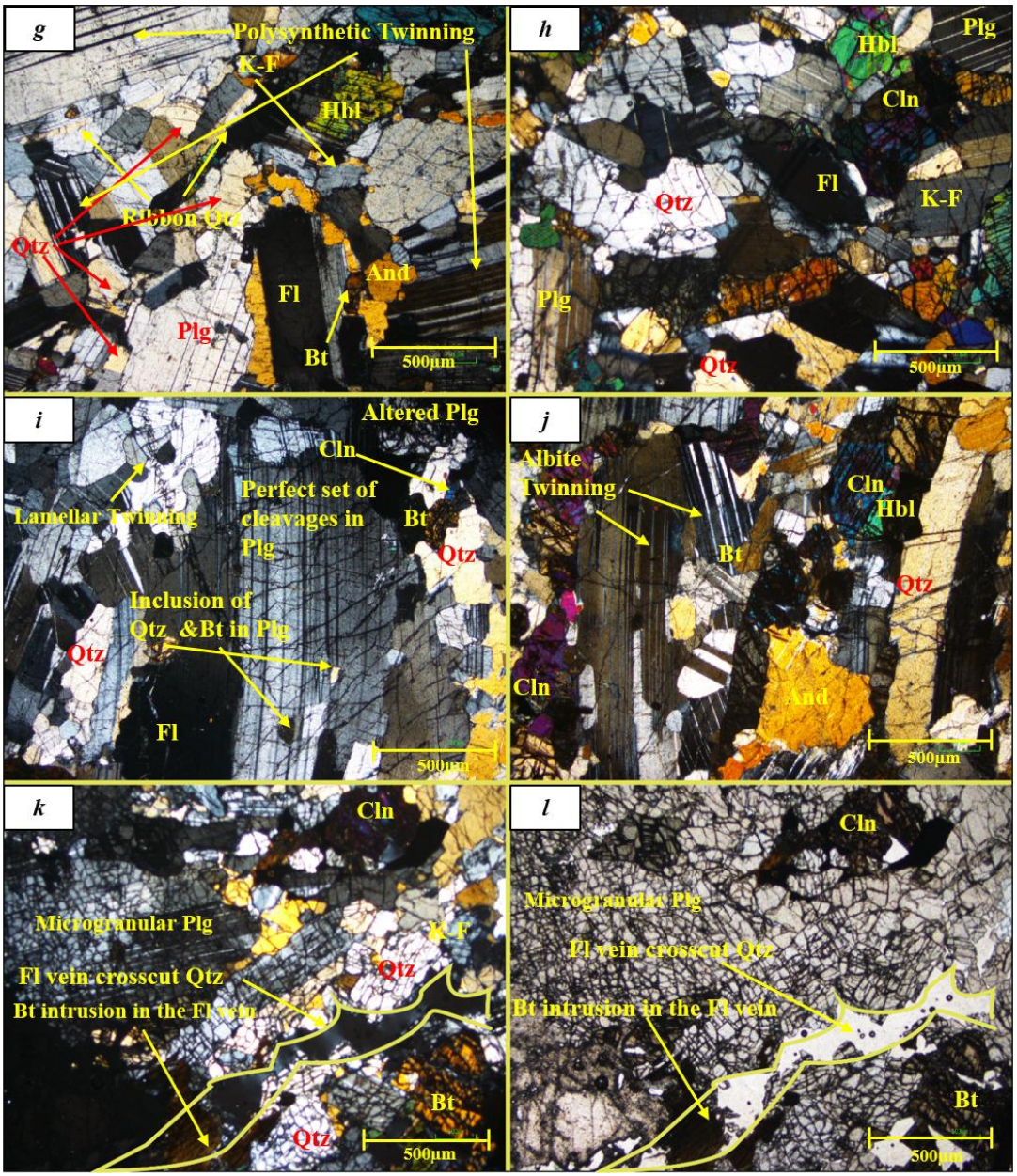

Fig. 4. ***Continued****. Photomicrographs illustrating (g) polysynthetic plagioclase and ribbon quartz, (h) quartz, hornblende, clinopyroxene, (i) perfect set of cleavages in plagioclase, Lameller Twinning and altered plagioclase, (j) Albite Twinning and clinopyroxene in contact with hornblende, (k) micro granular plagioclase, fluorite vein cross-cut quartz and biotite intrusion in the fluorite veins (XPL), (l) PPL view of micro granular plagioclase and fluorite veins*

Tab. 1. Model mineralogical concentrations of studied thin sections in percentages

Sample	Plg	Qtz	K-F	Bt	Hbl	Ms	Cln	And	Zr	Fl	Rt	Act
SK-1	44.75	22	7.5	7.75	0	0.5	4	9.25	0	0	3.75	0.5
SK-3	20	21.75	6.25	10.5	0	7.5	6	0	8.25	19.75	0	0
SK-5	35	22.25	10.75	10.25	9.5	1.75	3	4.25	0	3.25	0	0
SK-8	34.25	18.75	9.25	9.75	7.5	3	7.75	3.75	5	0	1	0
SK-9	29.25	22.75	8.5	9.75	7.25	5.25	5.75	2	0	9	0.5	0
SK-10	36.25	20.25	12.25	10.25	3.5	3.25	4.5	5.75	1	1	2	0
SK-12	31.75	26.75	9	8	2.5	2.75	6	12.75	0	0	0.5	0
SK-13	38.5	22.25	11.75	10.25	3	2.25	3.5	5.5	0	2	1	0
SK-15	37.75	24.25	7.75	9.25	5.5	4.25	3.25	4.5	0	2.25	1.25	0
SK-16	24.5	21.5	14.25	15.25	2.25	4.5	7.75	0	0	9.25	0.75	0

Physical and Mechanical Properties

Grading

This method is used to distribute the rock samples based on particle size. Grading is the basic analysis used to classify coarse and fine aggregates. The grading analysis results declare coarse sand aggregates as they are not passing from the 0.600mm sieve (Tab. 2).

Tab. 2. Results of sieve analysis.

Sample ID	Sieve No.	Total weight	Retained Weight	Retained %	Passing %
SK 1	No.4	1128.1g	1103.5g	97	3
	No.8	1128.1g	1112.9g	98	2
	No.16	1128.1g	1114.3g	98	2
	No.30	1128.1g	Not Passing	-	-
	No.50	1128.1g	Not Passing	-	-
SK 3	No.4	835.3g	805.23g	96.4	3.8
	No.8	835.3g	811.91g	97.2	2.8
	No.16	835.3g	818.59g	98	2
	No.30	835.3g	Not Passing	-	-
	No.50	835.3g	Not Passing	-	-
SK 5	No.4	1027.31g	984.16g	95.8	4.2
	No.8	1027.31g	992.38g	96.6	3.4
	No.16	1027.31g	1001.63g	97.5	2.5
	No.30	1027.31g	Not Passing	-	-
	No.50	1027.31g	Not Passing	-	-
SK 8	No.4	975.32g	916.800g	94	6
	No.8	975.32g	942.16g	96.6	3.4
	No.16	975.32g	953.86g	97.8	2.2
	No.30	975.32g	Not Passing	-	-
	No.50	975.32g	Not Passing	-	-
SK 9	No.4	784.72g	744.70g	94.9	6.1
	No.8	784.72g	761.96g	97.1	2.9
	No.16	784.72g	770.59g	98.2	1.8
	No.30	784.72g	Not Passing	-	-
	No.50	784.72g	Not Passing	-	-
SK 10	No.4	624.40g	601.30g	96.3	3.7
	No.8	624.40g	606.92g	97.2	2.8
	No.16	624.40g	611.91g	98	2
	No.30	624.40g	Not Passing	-	-
	No.50	624.40g	Not Passing	-	-
SK 12	No.4	1145.4g	1088.13g	95	5
	No.8	1145.4g	1105.31g	96.5	3.5
	No.16	1145.4g	1114.47g	97.3	2.7
	No.30	1145.4g	Not Passing	-	-
	No.50	1145.4g	Not Passing	-	-
SK 13	No.4	1087.2g	1050.23g	96.6	3.4
	No.8	1087.2g	1063.28g	97.8	2.2
	No.16	1087.2g	1067.63g	98.2	1.8
	No.30	1087.2g	Not Passing	-	-
	No.50	1087.2g	Not Passing	-	-
SK 15	No.4	1010.7g	955.11g	95.4	4.6
	No.8	1010.7g	978.36g	96.8	3.2
	No.16	1010.7g	987.45g	97.7	2.3
	No.30	1010.7g	Not Passing	-	-
	No.50	1010.7g	Not Passing	-	-
SK 16	No.4	880.2g	845.87g	96.1	3.9
	No.8	880.2g	857.31g	97.4	2.6
	No.16	880.2g	864.35g	98. 2	1.8
	No.30	880.2g	Not Passing	-	-
	No.50	880.2g	Not Passing	-	-

Fineness modulus

The fineness modulus specifies the properties of the aggregates. Generally, the fineness modulus is directly related to the concrete aggregate strength (Sabih et al., 2016). The ASTM C33 range for fineness modulus is 2.3-3.2. The result of the fineness modulus falls within the specified limits of ASTM, so they can be used as aggregate for construction purposes (Tab. 3).

$$\mathbf{F.M} = \frac{\text{Sum of the retained percentage}}{100}$$

Specific Gravity

The design and construction of any structure using aggregates mainly depend on the specific gravity and absorption (You et al., 2009). Specific gravity provides an idea about the strength and quality of the aggregates; the aggregates with low specific gravity are weaker than those with higher specific gravity. The aggregates having a specific gravity ≥2.55 are suitable for heavy construction work (Blyth and de Freitas, 2017). The values of the specific gravity are within the specified limits (Tab. 3), so it can be used as construction material in heavy projects like dams, retaining walls, and highways.

Absorption

Absorption shows the strength of the aggregates as higher absorption of aggregates will usually be unsuitable for construction purposes. The absorption values of the granodiorite are within the admissible limit, so it can be used as a building stone (Tab. 3).

Tab. 3. Results of various Physico-mechanical analysis.

Sample ID	Texture	F.M	Dry Specific gravity	SSD Specific gravity	W.A%	Porosity %
SK-1	Medium	2.93	2.87	2.89	0.41	1.21
SK-3	Coarse	2.92	2.81	2.84	1.02	2.28
SK-5	Medium	2.90	2.86	2.87	0.49	1.39
SK-8	Coarse	2.88	2.80	2.83	1.09	2.06
SK-9	Coarse	2.90	2.73	2.76	1.41	2.88
SK-10	Medium	2.91	2.84	2.86	0.53	1.43
SK-12	Coarse	2.89	2.78	2.81	1.07	2.53
SK-13	Medium	2.93	2.9	2.92	0.37	0.83
SK-15	Coarse	2.90	2.76	2.80	1.13	2.76
SK-16	Coarse	2.92	2.83	2.85	0.75	1.83

Sample ID	F. I %	E. I %	LAAV %	Soundness %	UCS (Mpa)	UTS (Mpa)
SK-1	9.7	9.96	33.8	2.6	59.5	10.5
SK-3	10	11	35.2	3.1	47.21	8.3
SK-5	9.98	10.4	34.6	2.8	58.41	10.21
SK-8	10.23	11.2	35.3	2.85	53.3	9.7
SK-9	10.47	11.2	36.8	3.34	45.6	7.2
SK-10	10.13	11.4	34.8	2.92	54.4	9.7
SK-12	10.32	11.7	35.9	2.97	52.1	9.3
SK-13	9.31	9.64	33.4	2.51	61.17	11.41
SK-15	10.27	11.2	36.3	3.0	48.52	8.4
SK-16	9.95	10.3	34.9	2.9	49.37	8.7

Flakiness and Elongation Index

The workability and strength of the concrete can be strongly impacted by the particle shape of the aggregate. The ASTM limit for the coarse aggregates is 15% by weight (Khan et al., 2025). The value of the studied samples is within the range, so they are suitable for construction purposes (Tab. 3).

Los Angeles Abrasion

The Los Angeles measures the toughness, abrasion and resistance to grinding of an aggregate. A lower Los Angeles Abrasion value reflects higher aggregate competency and greater resistance to crushing and disintegration (Khan et al., 2025). The Los Angeles Abrasion value of the studied samples is within the range, so it is suitable for use in concrete and road fillers (Rahman et al., 2022) (Tab. 3).

Soundness

Soundness is the total amount of resistance to the weathering and freezing-thawing cycle. The soundness values of the rocks are within the range (Tab. 3), so it suggests that they can be used as a construction material where there is freezing and thawing and temperature change continuously, especially in hilly areas, glacial, mountainous ranges, dams, bridges due to their strong resistance to weathering, water, and chemical alteration.

Unconfined Compression Strength (UCS)

UCS is a basic mechanical analysis used to assess the stability of a structure under loads. It is the maximum applied stress that the rock can bear when subjected to one-directional strength. The stress is applied in the axial direction from top to bottom (Bell, 2007). The ranges of the UCS of the rocks fall in the moderate strong to strong category (Tab. 3). The bulk samples of the representative rocks were cored, and their strength was determined against the petrography to establish a relationship between petrographic features and mechanical properties. (Fig. 5).

Unconfined Tensile Strength (UTS)

The tensile strength of the rocks is the pulling force required to rupture a rock sample divided by the cross-sectional area of the sample (Adonay & Looyeh, 2019). Rocks have a very low tensile strength as they are more susceptible to rupture under loads than compression. The average UTS value is 8.54 MPa. (Tab. 3).

Discussion

In order to understand the influence of petrographic characteristics on the mechanical behaviour of the Mayar Granodiorite, a comprehensive regression analysis is conducted between mineralogical compositions and physico-mechanical parameters (Table. 4; Fig. 5a–z). The results reveal distinct mineralogical controls, grain-size dependencies, and textural impacts that collectively influence rock strength and durability.

A strong positive linear relationship was observed between plagioclase content and both uniaxial compressive strength (UCS) and uniaxial tensile strength (UTS) (Fig. 5a, b, c), indicating that plagioclase plays a key role in enhancing rock strength. This can be attributed to the interlocking nature of subhedral to anhedral plagioclase crystals, many of which display polysynthetic and Carlsbad twinning (Fig. 4a, i), providing structural coherence that resists stress propagation. This observation contrasts with the findings of Sajid et al. (2016), who reported a negative correlation between plagioclase and UCS in granitic rocks. The discrepancy is explained by the presence of secondary alteration, such as sericitization, in their samples, whereas the plagioclase in the Mayar granodiorite appears relatively fresh and unaltered, maintaining its structural integrity. In contrast, quartz and K-feldspar showed no clear relationship with UCS or UTS (Fig. 5d, e, i, j). Although quartz is generally known for its high strength, its contribution to the mechanical performance of the studied granodiorite appears limited due to its internal texture. Many quartz grains display undulose extinction, ribbon texture, and fractures (Fig. 4d, g), which serve as planes of weakness under applied stress. These features reduce the granodiorite's overall strength, even though quartz is typically considered a strong and durable mineral. The unstrained quartz grains are also present (Fig. 4h), but they are not abundant enough to offset the weakening effects of the strained ones. This finding deviates from studies such as Tuğrul and Zarif (1999), Sajid and Arif (2015), Khalil et al. (2015), and Asif et al. (2024), who observed a positive correlation between quartz and UCS in granitic rocks. The discrepancy highlights the importance of considering not only modal abundance but also crystal texture and internal strain. Similarly, K-feldspar, despite being present in moderate amounts, does not correlate with strength, likely due to its weak relief, limited intergrowth textures, and lower bond strength within the rock matrix (Fig. 4c, k). Mica showed a strong negative correlation with UCS and UTS (Fig. 5g, h). These minerals occur in flaky, platy forms and are commonly aligned along micro-shear zones or cleavage planes, which act as preferred pathways for crack propagation. Photomicrographs reveal their presence both as individual flakes and intrusions into vein structures (Fig. 4c), reducing cohesion and enhancing anisotropy. This behaviour is consistent with previous observations in amphibolitic rocks by Sajid and Arif (2009), reinforcing the role of mica as a structural weakness modifier.

Grain size also plays a critical role in determining mechanical performance. Coarse-grained granodiorite samples consistently exhibited lower UCS and UTS values compared to medium-grained samples (Table 3; Fig. 5v). The reduction in strength among coarse-grained varieties can be attributed to larger grain boundaries and a higher likelihood of micro-fracturing, which compromise the load-bearing network within the rock. This finding agrees with studies by Arif et al. (2015) for granitic rocks and Yasir et al. (2018) for sandstone, although it differs from Sajid and Arif (2015), who reported stronger behaviour in coarse-grained granites. The divergence varies due to differences in intergranular bonding, grain alignment, and cementation quality, all of which vary depending on local petrogenesis.

Further insight is gained by evaluating the interrelationships between physical durability indicators. Coarse-grained samples show higher values for absorption, porosity, Los Angeles Abrasion Value (LAAV), and soundness (Table 3), all of which negatively impact mechanical performance (Fig. 5s, t, u, y, z). These properties are directly related to textural openness and fracture density. Plagioclase, by contrast, shows negative correlations with absorption, porosity, LAAV, and soundness (Fig. 5o, p, q), further underscoring its positive contribution to durability. Specific gravity, which positively correlates with UCS and inversely correlates with porosity and absorption (Fig. 5l, w), supports the interpretation that denser samples with tighter packing yield better performance.

An important observation is the UCS: UTS ratio, which averaged 5.7:1 across the studied samples, lower than the standard empirical relationships of 8:1 (Brady and Brown, 2004) and 10:1 (Farmer, 1983). The lower ratio may be attributed to relatively higher tensile resistance or reduced compressive resistance resulting from the presence of micro cracks, mica alignment, or heterogeneities in mineral orientation and texture. It also suggests that the rocks may behave less brittle in tensile failure than typically expected. Overall, the integrated analysis indicates that particularly plagioclase content, grain size, and microstructural features are the dominant factors controlling mechanical performance in the Mayar Granodiorite. The weak or neutral contributions of quartz and K-feldspar reflect the importance of textural condition over bulk abundance. The contrast between these findings and those of previous studies stems from differences in strain textures, mineral alteration, and rock fabric heterogeneity, emphasizing the need for site-specific evaluations in engineering geology. These findings clearly explain the conditions under which granodiorite can serve as high-performance aggregates and dimension stones for critical infrastructure projects.

Tab. 4. Relationship between minerals contents and mechanical properties.

Sample	Plg	Qtz	K-F	Bt	Ms	S.G	W.A	LAAV	Soundness	UCS(Mpa)	UTS(Mpa)	UCS:UTS
SK-1	44.75	22	7.5	7.75	0.75	2.87	0.41	33.8	2.6	59.5	10.5	5.67:1
SK-3	20	21.75	6.25	10.25	7.5	2.81	1.02	35.2	3.1	47.21	8.3	5.69:1
SK-5	35	22.25	10.75	10.25	1.75	2.86	0.49	34.6	2.8	58.41	10.2	5.73:1
SK-8	34.25	18.75	9.25	9.75	3	2.80	1.09	35.3	2.85	53.3	9.7	5.49:1
SK-9	29.25	22.75	8.5	9.75	5.25	2.73	1.41	36.8	3.34	45.6	7.2	6.33:1
SK-10	36.25	20.25	12.25	10.25	3.25	2.84	0.53	34.8	2.92	54.4	9.7	5.61:1
SK-12	31.75	26.75	9	8	2.75	2.78	1.07	35.9	2.97	52.1	9.3	5.6:1
SK-13	38.5	22.25	11.75	10.25	2.25	2.9	0.37	33.4	2.51	61.7	11.41	5.41:1
SK-15	37.75	24.25	7.75	9.25	4.25	2.76	1.13	36.3	3.0	48.52	8.4	5.78:1
SK-16	24.5	21.5	14.25	15.25	4.5	2.83	0.75	34.9	2.9	49.37	8.7	5.67:1

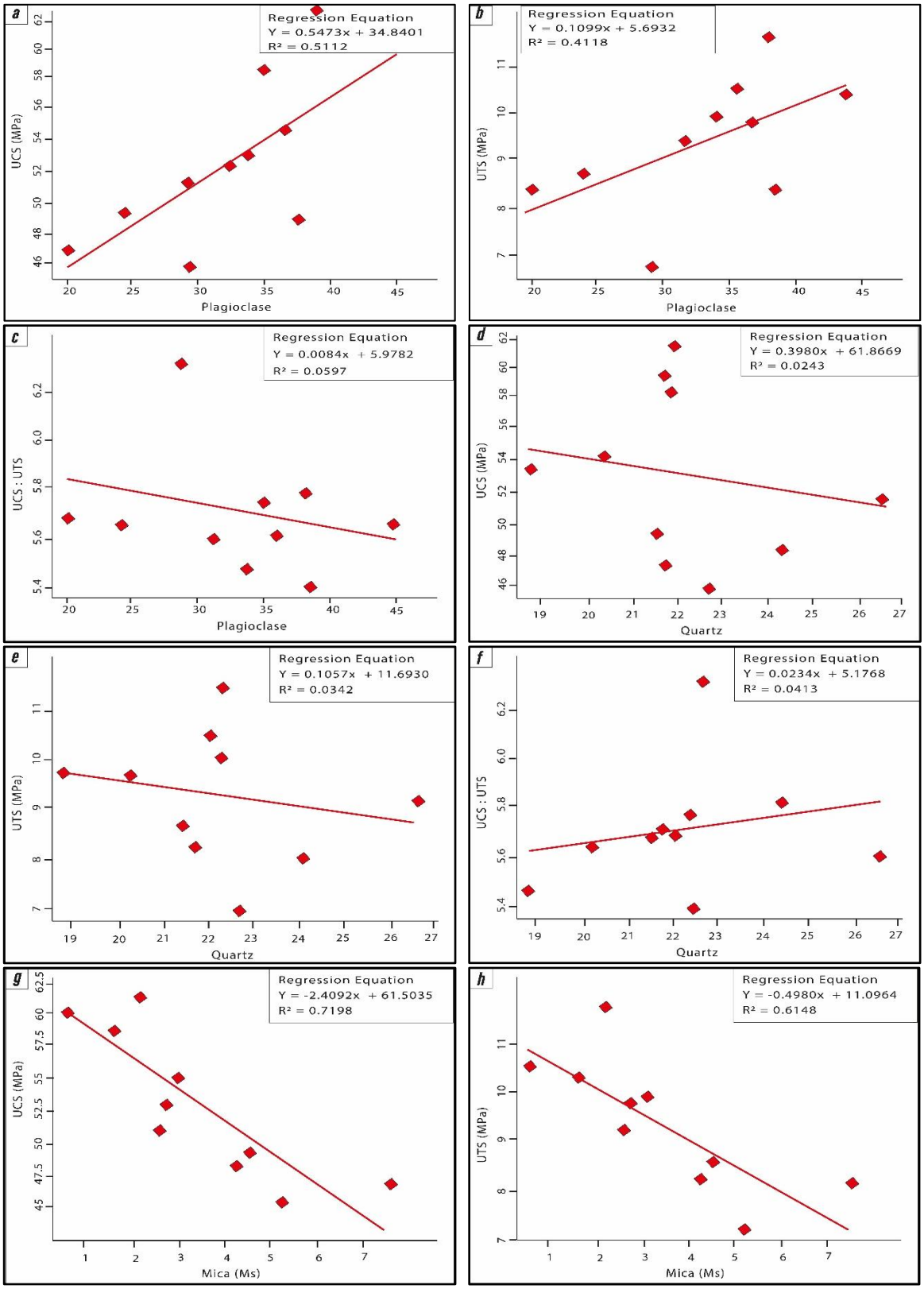

Fig. 5. Regression Analysis showing (a) a positive trend line between plagioclase and UCS, (b) a positive trend line between plagioclase and UTS, (c) no significant relationship between plagioclase and UCS: UTS, (d) no significant relationship between quartz and UCS, (e) no significant relationship between quartz and UTS, (f) no significant relationship between quartz and UCS: UTS, (g) negative trend line between Mica content and UCS, (h) negative trend line Mica content and UTS

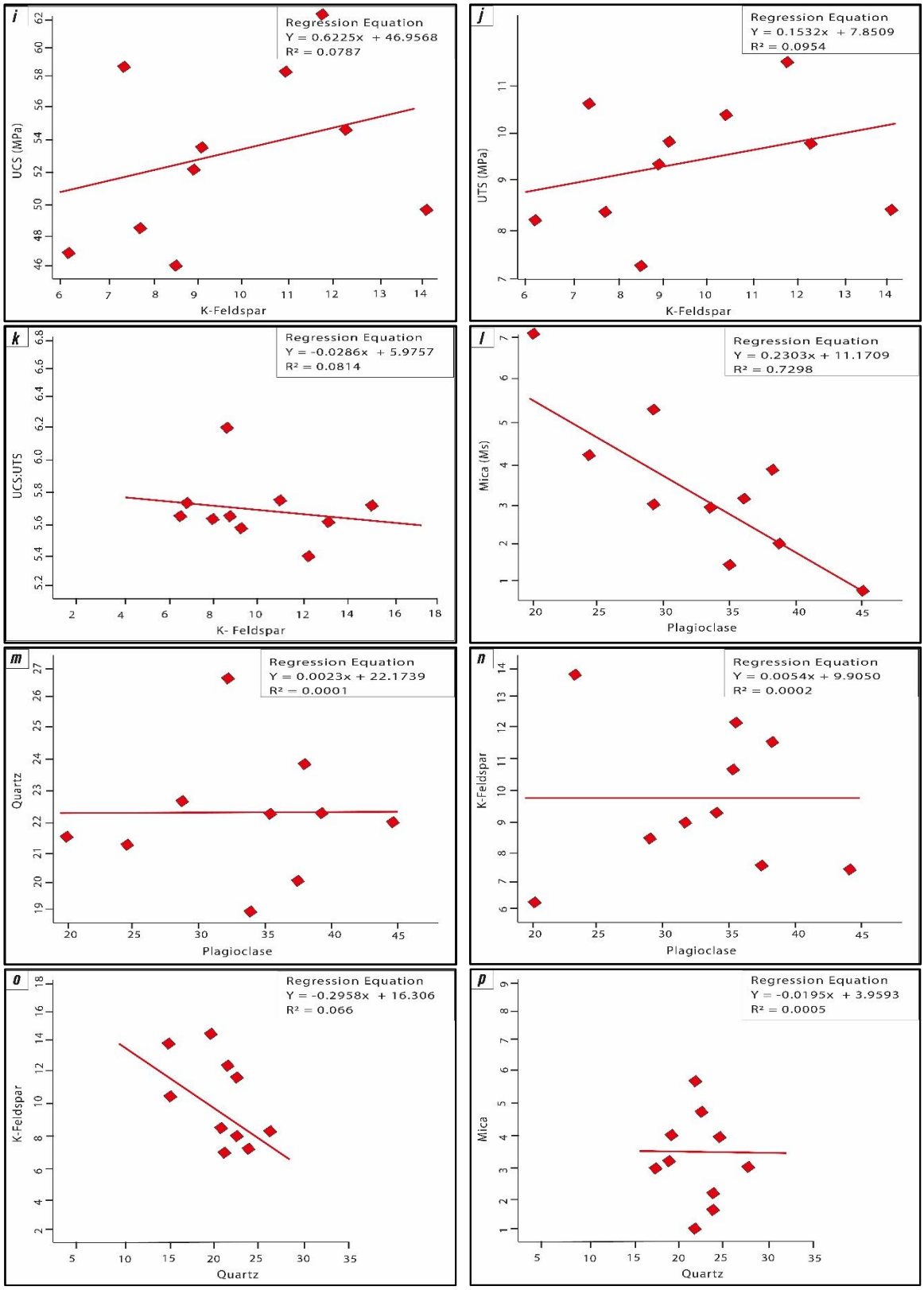

Fig. 5. Continued.. Regression Analysis showing (i) no significant relationship between K-feldspar and UCS, (j) no significant relationship between K-feldspar and UTS, (k) no significant relationship between K-feldspar and UCS:UTS, (l) inverse relationship between plagioclase and mica, (m) no significant relationship between plagioclase and quartz, (n) no significant relationship between plagioclase and K-feldspar, (o) negative trend line between quartz and K-feldspar (p) no significant relationship between quartz and mica

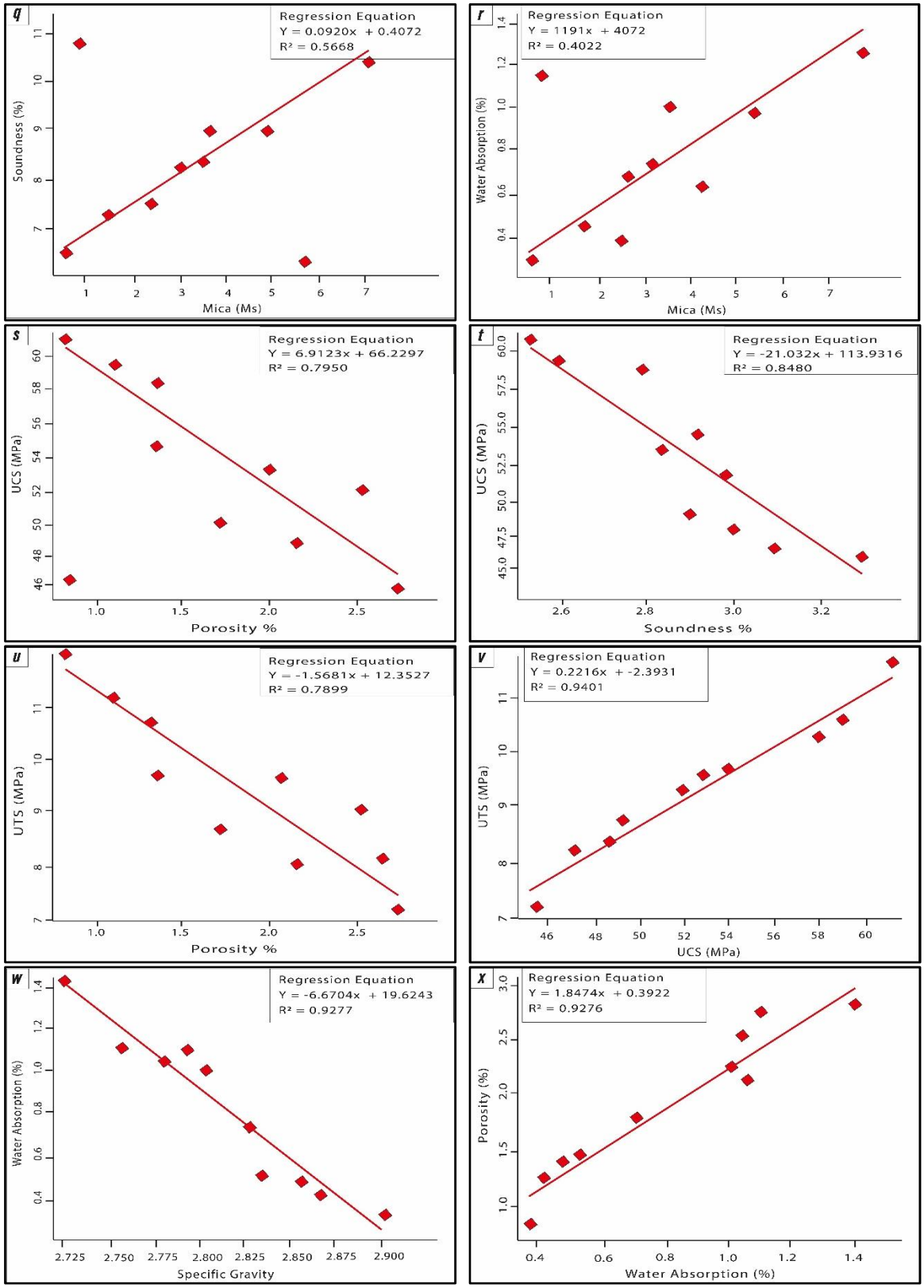

Fig. 5 Continued. Regression Analysis showing (q) positive trend line between mica and soundness, (r) direct relationship between mica and absorption, (s) negative trend line between porosity and UCS, (t) negative trend line between soundness and UCS, (u) negative trend line between porosity and UTS, (v) positive trend line between UCS and UTS, (w) inverse relationship between specific gravity and absorption, (x) direct relationship between absorption and porosity

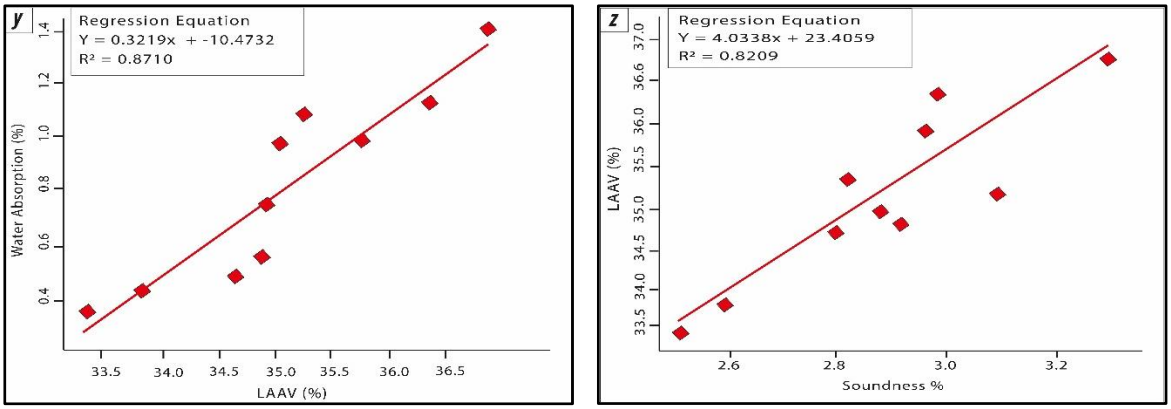

Fig. 5 Continued. Regression Analysis showing (y) positive trend line between LA Abrasion and absorption, (z) a positive trend line between soundness and LA Abrasion

Conclusion

The petrographic and physico-mechanical properties of granodiorite from Mayar Dir (Lower), Pakistan, were investigated, leading to the following conclusions. Petrographic analysis reveals that the granodiorite consists of plagioclase, K-feldspar, quartz, hornblende, biotite, and andalusite, with minor amounts of rutile, muscovite, zircon, and fluorite. The physico-mechanical properties of the granodiorite fall within ASTM limits, indicating its suitability as a construction material. The average UCS values of the selected core samples range from 49.37 MPa to 59.5 MPa, categorizing them as moderately strong. Coarse-grained granodiorite exhibits lower UCS and UTS values, along with higher absorption, porosity, Los Angeles abrasion, and soundness values, which can be attributed to the increased tendency for fracture formation in the coarse-grained material. The correlation between petrographic and physico-mechanical features shows that plagioclase is the dominant mineral responsible for the rock's strength, followed by quartz and K-feldspar. Mica flakes, on the other hand, display an inverse relationship with rock strength. The relationship between quartz and strength is complex, as it is influenced by the texture of quartz and its interaction with other minerals. These findings suggest that the granodiorite from the Mayar area is a viable option for use as coarse aggregate and dimension stone in construction projects such as roads, road fillers, dams, highways, bridges, tunnelling, and hydropower projects. Additionally, further investigation into the specific properties of quartz in relation to strength may help refine its role in determining the overall strength of granodiorite.

References

Adomako, S., Engelsen, C. J., Thorstensen, R. T., & Barbieri, D. M. (2021). Review of the relationship between aggregates geology and Los Angeles and micro-Deval tests. *Bulletin of Engineering Geology and the Environment*, *80*(3), 1963-1980. https://doi.org/10.1007/s10064-020-02097-y

Ahmad, I., Jan, M. Q., & DiPietro, J. A. (2003). Age and Tectonic implications of granitoid rocks from the Indian plate of Northern Pakistan. *J. Virt. Explorer, Electronic Edition*, *11*(2). https://doi.org/10.3809/jvirtex.2003.00066

Aman, k., Abbas, Z., & Waheed, A. (2025). Socioeconomic impacts of the 2022 floods on pakistan: an analysis. *Sociology & Cultural Research Review*, *3*(01), 779-799. https://doi.org/10.1097/MS9.0000000000002402

Arif, M., Islam, I., & Rizwan, M. (2015). Petrography and physico-mechanical properties of the granitic rocks from Kumrat valley, Kohistan Batholith, NW Pakistan. *AshEse Journal of Physical Science*, *1*(1), 1-8.

Asif, A. R., Islam, I., Ahmed, W., Sajid, M., Qadir, A., & Ditta, A. (2022). Exploring the potential of Eocene carbonates through petrographic, geochemical, and geotechnical analyses for their utilization as aggregates for engineering structures. *Arabian Journal of Geosciences*, *15*(11), 1105. https://doi.org/10.1007/s12517-022-10383-0

Asif, A. R., Shah, S. S. A., & Khan, J. (2021). The New Empirical Formulae for predicting the Unconfined Compressive Strength of limestone from Kohat Basin, Pakistan. *Journal of Himalayan Earth Sciences*, *54*(1), 33.

Asif, A. R., Sajid, M., Ahmed, W., Nawaz, A. (2024). Weathering effects on granitic rocks in North Pakistan: petrographic insights, strength classifications, and construction suitability. *Environmental Earth Sciences*, *83*, 351. https://doi.org/10.1007/s12665-024-11655-6

Attewell, P. B., & Farmer, I. W. (2012). *Principles of engineering geology*. Springer Science & Business Media. http://doi.org/10.1007/978-04-009-5707-7

Baig, S. S., Xue, C., Jan, M. Q., & Rehman, H. U. (2021). Late Jurassic adakite- like granodiorite along the southern Karakoram block, NE Pakistan: New evidence for subduction initiation of the Neo-Tethys Ocean. *Lithos*, *406*, 106496. https://doi.org/10.1016/j.lithos.2021.106496

Blyth, F. G. H., & De Freitas, M. (2017). *A Geology for Engineers*. CRC Press. https://doi.org/10.1201/9781315276113

Brady, B. H., & Brown, E. T. (2006). *Rock Mechanics: for underground mining*. Springer science & business media. https://doi.org/10.1007/978-1-4020-2116-9

Farmer, I. (1983). Rock Strength and Yield. In *Engineering Behaviour of Rocks* (pp. 81-118). Dordrecht: Springer Netherlands. http://doi.org/10.1007/978-94-009-5753-4

Hu, H., & Stern, R. J. (2020). Early Cretaceous subduction initiation beneath southern Tibet caused the northward flight of India. *Geoscience Frontiers*, *11*(4), 1123-1131. https://doi.org/10.1016/j.gsf.2020.01.010

Hussain, J., Zhang, J., Lina, X., Hussain, K., Shah, S. Y. A., Ali, S., & Hussain, A. (2022). Resource assessment of limestone based on engineering and petrographic analysis. *Civil Engineering Journal*, *8*(3), 421-437. http://dx.doi.org/10.28991/CEJ-2022-08-03-02

Kazmi, A. H., & Jan, M. Q. (1997). Geology and tectonics of Pakistan.

Khalil, Y. S., Arif, M., Bangash, H. A., Sajid, M., & Muhammad, N. (2015). Petrographic and structural controls on geotechnical feasibility of dam sites: implications from investigation at Sher Dara area (Swabi), north-western Pakistan. *Arabian Journal of Geosciences*, *8*, 5067-5079. https://doi.org/10.1007/s12517-014-1510-z

Khan, M. A., Stern, R. J., Gribble, R. F., & Windley, B. F. (1997). Geochemical and isotopic constraints on subduction polarity, magma sources, and palaeogeography of the Kohistan intra-oceanic arc, northern Pakistan Himalaya. *Journal of the Geological Society*, *154*(6), 935-946. https://doi.org/10.1144/gsjgs.154.6.0935

Khan, R., Siyar, S. M., Naseem, A. A., Ullah, F., Bilal, M., Hussain, M., Bilal, M., & Shahab, M.: 2025. Integrated petrographic, geochemical and mechanical evaluations of diorite rocks for sustainable aggregate usage: A case study from ZardAli Banda Area, Northern Pakistan. *Acta Geodynamica et Geomaterialia, 22(217)*, 105-120. http://doi.org/ 10.13168/AGG.2025.0008

Khattak, S. A., Qadir, A., Daud, H., Shehzad, K., Yasir, M., & Abubakar, M. (2021). Terrace soil suitability for highway construction: Case study in lesser Himalaya (CPEC project E-35), North Pakistan. *International Journal of Economic and Environmental Geology*, *12*(3), 54-59. https://doi.org/10.46660/ijeeg.v12i3.63

Maitre, L. (2002). Igneous rocks. A classification and glossary of terms. https://doi.org/10.1017/S0016756803388028

Nanditha, J. S., Kushwaha, A. P., Singh, R., Malik, I., Solanki, H., Chuphal, D. S.,& Mishra, V. (2023). The Pakistan flood of August 2022: causes and implications. *Earth's Future*, *11*(3). https://doi.org/10.1029/2022EF003230

Naseem, A. A., Anjum, M. N., Yaseen, M., Ali, M., Inam, W., Ali, S. H., & Bangash, A. A. (2023). Preliminary Geoheritage Assessment of The Gharam Chashma Granitic Batholith (GCGB), Southern Margin of Asian Plate, NW Pakistan: Multiple Constraints from Field Evidence, Petrology, and Physicomechanical Properties. *Geoheritage*, *15*(1), 31. https://doi.org/10.1007/s12371-023-00798-w

Petterson, M. G. (2010). A review of the geology and tectonics of the Kohistan island arc, north Pakistan. *Geological Society, London, Special Publications*, *338*(1), 287-327. https://doi.org/10.1144/SP338.14

Pichler, H., & Schmitt-Riegraf, C. (1997). *Rock-forming minerals in thin section*. Springer Science & Business Media. https://doi.org/10.1007/978-94-009-1443-8

Rahman, A. U., Zhang, G., Khan, A., Muhammad, J., Sohail, A., Rehman, H. U., & Ashraf, B. (2022). The Effect of Mineral Composition, Microstructure on Physical Properties of Aggregate from River Punjkora and Kunai, Dir (Lower), Khyber Pakhtunkhwa, Pakistan. *Journal of Geoscience and Environment Protection*, *10*(4), 127-144. http://doi.org/10.4236/gep.2022.104009

Rashid, A., Khan, S., Ayub, M., Sardar, T., Jehan, S., Zahir, S., Khan, S. K., Muhammad, J., Khan, R., Ali, A., & Ullah, H. (2019). Mapping human health risk from exposure to potential toxic metal contamination in groundwater of Lower Dir, Pakistan: Application of multivariate and geographical information system. *Chemosphere*, *225*, 785-795. https://doi.org/10.1016/j.chemosphere.2019.03.066

Sabih, G., Tarefder, R. A., & Jamil, S. M. (2016). Optimization of gradation and fineness modulus of naturally fine sands for improved performance as fine aggregate in concrete. *Procedia Engineering*, *145*, 66-73. https://doi.org/10.1016/j.proeng.2016.04.016

Shah, S. S. A., Turrakheil, K. S., & Naveed, M. (2024). Impact of Wetting and Drying Cycles on the Hydromechanical Properties of Soil and Implications on Slope Stability. Atmosphere, 15(11), 1368. https://doi.org/10.3390/atmos15111368

Sajid, M., & Arif, M. (2015). Reliance of physico-mechanical properties on petrographic characteristics: consequences from the study of Utla granites, north-west Pakistan. *Bulletin of Engineering Geology and the Environment*, *74*, 1321-1330. https://doi.org/10.1007/s10064-014-0690-9

Sajid, M., Arif, M., & Muhammad, N. (2009). Petrographic characteristics and mechanical properties of rocks from Khagram-Razagram area, Lower Dir, NWFP, Pakistan. *Journal of Himalayan Earth Sciences*, *42*, 25-36.

Sajid, M., Coggan, J., Arif, M., Andersen, J., & Rollinson, G. (2016). Petrographic features as an effective indicator for the variation in strength of granites. *Engineering Geology*, *202*, 44-54. https://doi.org/10.1016/j.enggeo.2016.01.001

Searle, M. P., Khan, M. A., Fraser, J. E., Gough, S. J., & Jan, M. Q. (1999). The tectonic evolution of the Kohistan-Karakoram collision belt along the Karakoram Highway transect, north Pakistan. *Tectonics*, *18*(6), 929-949. https://doi.org/10.1029/1999TC900042

Siegesmund, S., Wiese, F., Klein, C., Huster, U., & Pötzl, C. (2022). Weathering phenomena, rock physical properties and long-term restoration intervention: a case study from the St. Johannis Chapel of Lütgenrode (Lower Saxony, Germany). *Environmental Earth Sciences*, *81*(15), 389. https://doi.org/10.1007/s12665-022-10446-1

Sawa, J. N. (2023). New waves of flash floods and risks perception of climate change: an overview of the 2022 flood disaster in pakistan. *Pakistan Journal of Humanities and Social Sciences Research*, *6*(2), 72-82. https://doi.org/10.37605/pjhssr.v6i2.4

Tuğrul, A., & Zarif, I. H. (1999). Correlation of mineralogical and textural characteristics with engineering properties of selected granitic rocks from Turkey. *Engineering geology*, *51*(4), 303-317. https://doi.org/10.1016/S0013-7952(98)00071-4

Yasir, S. F., Awang, H., & Ayub, M. I. H. (2018). The relationship of sandstone's strength with mineral content and petrographic characteristics in Sungai Tekai, Jerantut, Pahang. In *AIP Conference Proceedings* (Vol. 2020, No. 1). AIP Publishing. https://doi.org/10.1063/1.5062636

You, Z., Adhikari, S., & Emin Kutay, M. (2009). Dynamic modulus simulation of the asphalt concrete using the X-ray computed tomography images. *Materials and Structures*, *42*, 617-630. https://doi.org/10.1617/s11527-008-9408-4

Ullah, F., Hussain, M., Siyar, S. M., Khan, R., Naseem, A.A., Jalil, R., Alshehri, F., & Shahab M. (2025). Petrogenetic study of diorite and Fe-Mg diorite from the Samar Bagh Complex: Insights from petrographic and Geochemical Analyses. *Acta Geodynamica et Geomaterialia, 22(217)*, 87-104. http://doi.org/10.13168/AGG.2025.0007